CERTS Project

Voltage Stability Applications using Synchrophasor Data

Report 3

Development of the Voltage Stability Analysis Framework

Submitted by

Joe H. Chow and Scott G. Ghiocel

Rensselaer Polytechnic Institute
110 8th Street
Troy, NY 12180-3590

December 5, 2013

Prepared for

Dejan Sobajic, Project Manager

Office of Electricity Delivery and Energy Reliability Transmission Reliability Program of the U.S. Department of Energy Under Contract No. DE-AC02-05CH11231

Acknowledgement

The work described in this paper was coordinated by the Consortium for Electric Reliability Technology Solutions, and funded by the Office of Electricity Delivery and Energy Reliability, Transmission Reliability Program of the U.S. Department of Energy through a contract with Rensselaer Polytechnic Institute administered by the Lawrence Berkeley National Laboratory. This work was supported by the Lawrence Berkeley National Lab (LBL) subcontract 7040520 of prime contract DE-AC02-05CH11231 between LBL and Department of Energy (DOE). The authors gratefully acknowledge the support provided by Lawrence Berkeley National Lab (LBL) and Department of Energy (DOE).

Disclaimer

This document was prepared as an account of work sponsored by the United States Government. While this document is believed to contain correct information, neither the United States Government nor any agency thereof, nor The Regents of the University of California, nor any of their employees, makes any warranty, express or implied, or assumes any legal responsibility for the accuracy, completeness, or usefulness of any information, apparatus, product, or process disclosed, or represents that its use would not infringe privately owned rights. Reference herein to any specific commercial product, process, or service by its trade name, trademark, manufacturer, or otherwise, does not necessarily constitute or imply its endorsement, recommendation, or favoring by the United States Government or any agency thereof, or The Regents of the University of California. The views and opinions of authors expressed herein do not necessarily state or reflect those of the United States Government or any agency thereof, or The Regents of the University of California.

A Power Flow Method using a New Bus Type for Computing Steady-State Voltage Stability Margins

Scott G. Ghiocel, *Student Member, IEEE* and Joe H. Chow, *Fellow, IEEE*

***Abstract*—In steady-state voltage stability analysis, it is well-known that as the load is increased toward the maximum loading condition, the conventional Newton-Raphson power flow Jacobian matrix becomes increasingly ill-conditioned. As a result, the power flow fails to converge before reaching the maximum loading condition. To circumvent this singularity problem, continuation power flow methods have been developed. In these methods, the size of the Jacobian matrix is increased by one, and the Jacobian matrix becomes non-singular with a suitable choice of the continuation parameter.**

In this paper, we propose a new method to directly eliminate the singularity by reformulating the power flow. The central idea is to introduce an AQ bus in which the bus angle and the reactive power consumption of a load bus are specified. For steady-state voltage stability analysis, the voltage angle at the load bus can be varied to control power transfer to the load, rather than specifying the load power itself. For an AQ bus, the power flow formulation consists of only the reactive power equation, thus reducing the size of the Jacobian matrix by one. This reduced Jacobian matrix is nonsingular at the critical voltage point. We illustrate the method and its application to steady-state voltage stability using two example systems.

***Index Terms*—Voltage stability analysis, voltage stability margin, Jacobian singularity, angle parametrization, AQ bus**

I. Introduction

Voltage instability has been the cause of many major blackouts [1, 2, 3]. In a power system operation environment, it is important to ensure that the current operating condition is voltage stable subject to all credible contingencies. Methods for calculating the stability margin for each contingency can be classified into two categories: dynamic (time-domain simulation) and steady-state (power flow methods) [4, 5]. Time-domain simulation can capture the dynamic elements of voltage instability. In this paper we are only dealing with steady-state voltage stability analysis occurring over a long time span.

One difficulty in steady-state voltage stability analysis is that the conventional Newton-Raphson power flow fails to converge as the maximum loadability point is reached. In the unconstrained case, the Jacobian matrix J becomes singular at maximum loading, and the power flow solution will not converge when the smallest singular value of J becomes too small [4, 5].

To circumvent this singularity problem, continuation power flow methods based on homotopy techniques have been developed [6, 7]. In this approach, a load-increase continuation parameter λ is introduced as an additional variable. As a result, the size of the Jacobian matrix is increased by one, which becomes non-singular with a suitable choice of the continuation parameter. The continuation power flow is solved in a two-step process with a predictor step and a corrector step, and requires additional manipulations and computation [8]. During the corrector step, the continuation method still needs to deal with a poorly conditioned Jacobian.

Table I
POWER FLOW BUS TYPES

Bus types	Bus representation	Fixed values
PV	Generator buses	Active power generation and bus voltage magnitude
PQ	Load buses	Active and reactive consumption
AV	Swing bus	Voltage magnitude and angle
AQ	Load buses	Voltage angle and reactive power consumption

In this paper, we propose a new power flow method to directly eliminate the singularity issue without adding the additional complexity required by such homotopy methods. Elimination of the singularity allows for a well-conditioned power flow solution even at the maximum loadability point. The central idea is to reformulate the power flow with the introduction of a new type of load bus, which we call an AQ bus (A stands for angle). A conventional power flow formulation uses three types of buses: PV buses, PQ buses, and the swing bus (Table I[1]). For an AQ bus, the bus voltage angle θ and the reactive power consumption Q are specified. In this sense, a swing bus can be considered as an AV bus, because its angle is fixed and its voltage magnitude is known. In this formulation, the active power balance equation at the AQ load bus is no longer needed. Only the reactive power balance equation is kept. Furthermore, because θ at this bus is known, it is eliminated from the power flow solution vector consisting of bus voltage magnitudes of PQ buses and bus voltage angles of all the buses except for the swing bus. Thus the size of the resulting Jacobian matrix J_R is reduced by one. This J_R matrix is nonsingular at the maximum loadability point, and thus it avoids the singularity problem of the conventional Jacobian matrix J.

The load increase on Bus B_L, when specified as an AQ bus in this new power flow method, is achieved by increasing the bus voltage angle separation θ_s between Bus B_L and the swing bus. It is expected that the load P_L will increase with θ_s until

S. Ghiocel and J. Chow are with the Department of Electrical, Computer, and Systems Engineering, Rensselaer Polytechnic Institute, Troy, NY 12180, USA. (e-mail: ghiocel@alum.rpi.edu, chowj@rpi.edu)

[1]A recent paper [9] lists 16 bus types, of which the AQ or θQ bus is one of them. The paper addresses only the solvability issue of the Bus-type Extended Load Flow (BELF), without addressing specifically the voltage stability margin calculation using the AQ-bus formulation.

the critical voltage point, then further increases in θ_s will result in a decrease of P_L. For each value of θ_s, the amount of P_L is not known until the power flow is solved. This eliminates the active power balance equation at the load bus B_L. The reactive power balance equation at B_L is still maintained. For load increases involving constant-power-factor loads and at multiple buses, additional expressions are needed to develop the reduced Jacobian matrix J_R. The computation of voltage stability margins using this method is no more complicated than a conventional load flow solution and the step size in increasing θ to reach the critical voltage point is not limited. In addition, computation-speed enhancement techniques such as decoupled power flow can still be used [10].

This paper is organized as follows. In Section II, we use a single-load stiff-bus model to motivate the new problem formulation. Sections III provides the general framework of the approach. Section IV uses two example test systems to illustrate the method.

II. Motivation

Consider the two-bus power system shown in Fig. 1, in which the load bus is connected via a reactance X to the stiff voltage source with $E = 1$ pu and its angle set to zero. The load is denoted by a voltage of magnitude V_L and phase $-\theta_s$, and a power consumption $P_L + jQ_L$. The angle θ_s is positive so that power is transferred from the stiff source to the load. Following [4], we will consider the power flow solutions of the system for constant power load where $Q_L = P_L \tan(\phi)$, where $\cos(\phi)$ is the power factor (ϕ is positive for lagging and negative for leading).

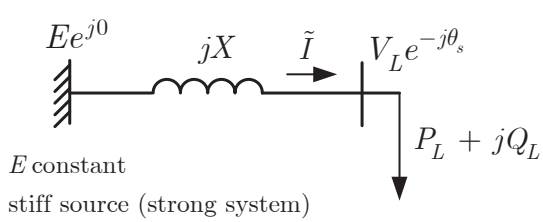

Figure 1. A two-bus power system

There are two relevant power flow equations for this system, both for the load bus:

$$P_L = -\frac{V_L E \sin\theta_s}{X}, \quad Q_L = \frac{V_L E \cos\theta_s}{X} - \frac{V_L^2}{X} \tag{1}$$

Treating the load bus as a PQ bus, the Jacobian matrix obtained by taking the partial derivatives of these two equations with respect to θ_s and V_L is

$$J = -\frac{1}{X}\begin{bmatrix} V_L E\cos\theta_s & E\sin\theta_s \\ V_L E\sin\theta_s & 2V_L - E\cos\theta_s \end{bmatrix} \tag{2}$$

The Jacobian J is singular when

$$\det J = (2V_L\cos\theta_s - E)/X = 0 \tag{3}$$

which occurs at the critical voltage point.

If the load bus is taken as an AQ bus, then the separation angle θ_s can be specified without specifying P_L and the active power equation is no longer needed. If Q_L is fixed, then the reduced matrix J_R is simply the (2,2) entry of J (2). Here the load is of constant power factor, i.e., $Q_L = P_L \tan\phi$, allowing the reactive power equation to be rewritten as

$$Q_L = \frac{V_L E\cos\theta_s}{X} - \frac{V_L^2}{X} = -\frac{V_L E\sin\theta_s}{X}\tan\phi \tag{4}$$

that is,

$$0 = \frac{V_L E\cos\theta_s}{X} - \frac{V_L^2}{X} + \frac{V_L E\sin\theta_s}{X}\tan\phi \tag{5}$$

The reduced Jacobian is the partial derivative of (5) with respect to V_L

$$J_R = \frac{1}{X}(E\cos\theta_s - 2V_L + E\sin\theta_s\tan\phi) \tag{6}$$

which is singular when $J_R = 0$.

For the 2-bus system in Fig. 1, we explore the singularities of the Jacobians (2) and (6). Using $E = 1$ pu and $X = 0.1$ pu, we plot the variation of θ_s, P_L, V_L, and the determinants of J and J_R, for 0.9 lagging, unity, and 0.9 leading power factor loads. Fig. 2 shows the familiar PV curve. The singularity of J occurs when the slope of the PV curve becomes infinite.

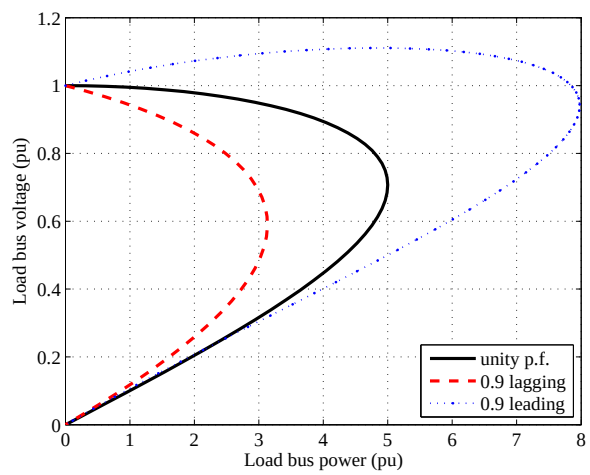

Figure 2. PV curves

Figs. 3 and 4 show the variation of V_L and P_L versus θ_s. The slopes of these curves are finite within the complete operational range of the angle separation. The peak of each P_L curve in Fig. 4 corresponds to the value of the separation angle θ_c at the critical voltage point. Note that the power factor of the load determines the maximum θ_s that is feasible.

The values of the determinants of J and J_R are shown in Fig. 5. It is obvious that $\det(J) = 0$ at θ_c, the value of the angle separation at the critical voltage point. On the other hand, J_R remains nonzero at θ_c, such that the Newton-Raphson iteration scheme will readily converge. In addition, $J_R = 0$ only when the load bus voltage V_L is zero.

Figs. 4 and 5 show that the separation angle θ_s is a useful variable to provide additional insights into the voltage stability problem. Most voltage stability analysis investigations have focused directly on V_L and largely ignored following up on θ_s.

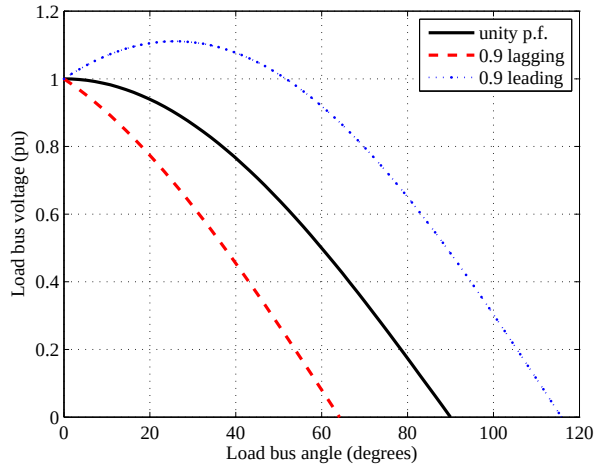

Figure 3. Variation of V_L versus θ_s

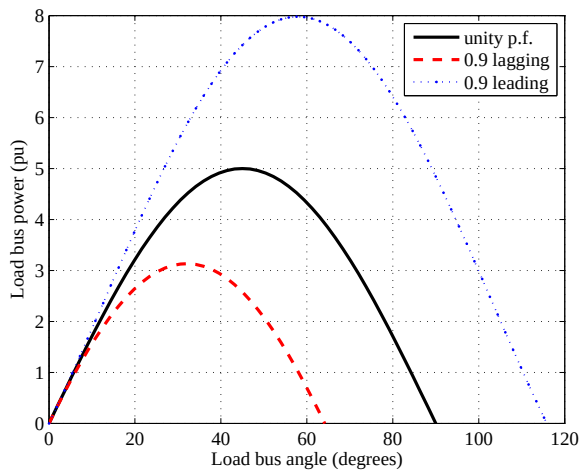

Figure 4. Variation of P_L versus θ_s

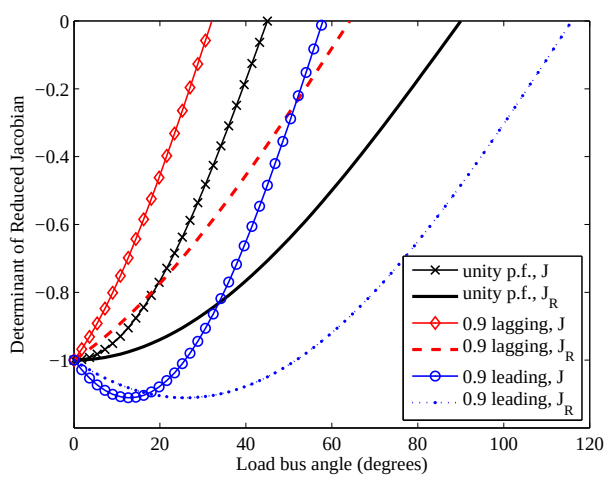

Figure 5. Determinant of J and J_R as a function of θ_s

III. Theoretical Framework and Computation Algorithms

In this section, we consider the general framework of a power flow formulation including an AQ bus, and extend the method for steady-state voltage stability analysis allowing for load and generation increases on multiple buses and for constant power factor loads.

Consider a power system with N_G generator buses and N_L load buses, such that the total number of buses is $N = N_G + N_L$. Let Bus 1 be the swing bus, Buses 2 to N_G be the generator PV buses, and Buses N_G+1 to N be the load PQ buses.

The power flow problem consists of solving the active and reactive power injection balance equations

$$\Delta P_i = P_i - f_{Pi}(\theta, V) = 0, \quad i = 2, ..., N \tag{7}$$

$$\Delta Q_i = Q_i - f_{Qi}(\theta, V) = 0, \quad i = N_G + 1, ..., N \tag{8}$$

where P_i and Q_i are the scheduled active and reactive power injections at Bus i. Vectors V and θ contain the bus voltage magnitudes and angles, and $f_{Pi}(\theta, V)$ and $f_{Qi}(\theta, V)$ are the computed active and reactive power injections, respectively. ΔP is the vector of active power mismatches at Buses 2 to N, and ΔQ is the vector of reactive power mismatches at Buses $N_G + 1$ to N.

The power flow problem is commonly solved by the Newton-Raphson method, using the iteration

$$J \begin{bmatrix} \Delta\theta \\ \Delta V \end{bmatrix} = \begin{bmatrix} J_{11} & J_{12} \\ J_{21} & J_{22} \end{bmatrix} \begin{bmatrix} \Delta\theta \\ \Delta V \end{bmatrix} = \begin{bmatrix} \Delta P \\ \Delta Q \end{bmatrix} \tag{9}$$

where the Jacobian matrix J is a square matrix of dimension $(2N - N_G - 1)$ containing the partial derivatives of the active and reactive power flow equations with respect to the bus angles θ and the voltage magnitudes V, where

$$J_{11} = \frac{\partial f_P}{\partial \theta}, \; J_{12} = \frac{\partial f_P}{\partial V}, \; J_{21} = \frac{\partial f_Q}{\partial \theta}, \; J_{22} = \frac{\partial f_Q}{\partial V} \tag{10}$$

$$\theta = \begin{bmatrix} \theta_2 & \cdots & \theta_N \end{bmatrix}^{\mathrm{T}} \tag{11}$$

$$V = \begin{bmatrix} V_{N_G+1} & \cdots & V_N \end{bmatrix}^{\mathrm{T}} \tag{12}$$

$\Delta\theta$ and ΔV are the corrections on θ and V, respectively.

A. Power flow formulation including an AQ bus

Suppose Bus N is an AQ bus with $\theta_N = \theta_N^\circ$ and Q_N specified, then the Newton-Raphson iteration reduces to

$$J_R \begin{bmatrix} \Delta\theta_R \\ \Delta V \end{bmatrix} = \begin{bmatrix} J_{R11} & J_{R12} \\ J_{R21} & J_{R22} \end{bmatrix} \begin{bmatrix} \Delta\theta_R \\ \Delta V \end{bmatrix} = \begin{bmatrix} \Delta P_R \\ \Delta Q \end{bmatrix} \tag{13}$$

where

$$J_{R11} = J_{11}(1 \ldots N-2; 1 \ldots N-2)|_{\theta_N = \theta_N^\circ} \tag{14}$$

$$J_{R12} = J_{12}(1 \ldots N-2; 1 \ldots N-N_G)|_{\theta_N = \theta_N^\circ} \tag{15}$$

$$J_{R21} = J_{21}(1 \ldots N-N_G; 1 \ldots N-2)|_{\theta_N = \theta_N^\circ} \tag{16}$$

$$J_{R22} = J_{22}|_{\theta_N = \theta_N^\circ} \tag{17}$$

The number of bus angle variables is reduced by one, such that

$$\Delta\theta_R = \begin{bmatrix} \Delta\theta_2 & \cdots & \Delta\theta_{N-1} \end{bmatrix}^{\mathrm{T}} \tag{18}$$

The AQ bus active power flow equation is eliminated, such that ΔP_R is the vector of active power mismatches at Buses 2 to $(N-1)$. The load P_N on Bus N is no longer specified, but it can be computed using $f_{Pi}(\theta, V)$.

This reduced power flow formulation would not yield directly a specific P_N on Bus N. However, this is not a hindrance in voltage stability analysis. Instead of increasing P_N on Bus N and not knowing whether the non-convergent result is actually the maximum loadability point, a user can keep increasing the angular separation between Bus N and the swing bus until the maximum power transfer point is reached. The reduced Jacobian J_R would not be singular at that point and the maximum loadability point can be readily computed.

B. Voltage stability analysis for constant-power-factor loads

In voltage stability analysis, it is common to specify constant-power-factor loads. In this section, we will extend the iteration (13) to a more general case by considering constant-power-factor load increases at multiple load buses to be supplied by generators at multiple locations.

Let Buses N_p to N be load buses with constant power factor $\cos\phi_\ell$, that is, $Q_\ell = P_\ell \tan\phi_\ell$ for $\ell = N_p, ..., N$. The active power load increases at these load buses are scaled with respect to Bus N, that is,

$$P_\ell - P_\ell^0 = \alpha_\ell \left(P_N - P_N^0\right), \quad \ell = N_p, ..., N-1 \tag{19}$$

The load increase is balanced by increases in outputs of generators on Buses 1 to q, with the active power at these generators scaled according to the swing bus

$$P_k - P_k^0 = \beta_k \left(P_1 - P_1^0\right), \quad k = 2, ..., q \tag{20}$$

In a solved power flow solution, the active power injections at Buses 1 and N are computed as the power flow leaving the buses on the lines interconnecting them to the other buses. Thus in an AQ-bus formulation, we account for the groups of increasing load and generation by modifying the power flow injection equations such that

$$f_{Pk}(V,\theta) = \beta_k f_{P1}(V,\theta), \quad k = 2, ..., q \tag{21}$$

$$f_{P\ell}(V,\theta) = \alpha_\ell f_{PN}(V,\theta), \quad \ell = N_p, ..., N-1 \tag{22}$$

$$f_{Q\ell}(V,\theta) = \alpha_\ell f_{PN}(V,\theta)\tan\phi_\ell, \quad \ell = N_p, ..., N-1 \tag{23}$$

The other injection equations remain unchanged.

In obtaining a new reduced Jacobian matrix to solve this new power flow problem, we need two row vectors of partial derivatives of f_{P1} and f_{PN}

$$J_i = \begin{bmatrix} \frac{\partial f_{Pi}}{\partial \theta_R} & \frac{\partial f_{Pi}}{\partial V} \end{bmatrix}, \qquad i = 1, N \tag{24}$$

where J_i is the ith row of the Jacobian. Note that J_N is row $N-1$ of J without the entry due to $\Delta\theta_N$, and J_1 is not contained in J because Bus 1 is the swing bus.

Thus the reduced Jacobian J_R in (13) for the fixed reactive power injection problem is modified to form a new reduced Jacobian $\bar{J}_R$, such that

$$\bar{J}_{Ri} = J_{Ri} - \beta_k J_1, \qquad i = 1, ..., q-1, \quad k = 2, ...q \tag{25}$$

$$\bar{J}_{Ri} = J_{Ri} - \alpha_\ell J_N, \qquad i = N_p - 1, ..., N-2, \quad \ell = N_p, ..., N-1 \tag{26}$$

$$\bar{J}_{Ri} = J_{Ri} - \alpha_\ell J_N \tan\phi_\ell, \quad i = N_{J_R} - N_p, ..., N_{J_R}, \quad \ell = N_p, ..., N-1 \tag{27}$$

where $N_{J_R} = 2N - N_G - 2$ is the dimension of J_R. The other rows of J_R remain unchanged.

In this more general formulation of the AQ-bus power flow, the Newton-Raphson iteration becomes

$$\bar{J}_R \begin{bmatrix} \Delta\theta_R \\ \Delta V \end{bmatrix} = \begin{bmatrix} \Delta P_R \\ \Delta Q \end{bmatrix} \tag{28}$$

where the power mismatch (21)-(23) is based on the previous iteration. In voltage stability margin calculations, the injection solution at a lower angle separation condition can be used to initiate the solution process.

C. Algorithms for computing voltage stability margins

Because $\bar{J}_R$ in (28) would not be singular at the maximum loadability point, fast and well-conditioned voltage stability margin calculation methods can be formulated. Here we present two algorithms for steady-state voltage stability analysis as basic applications of the AQ-bus method.

Algorithm 1: using AQ-bus power flow with $\bar{J}_R$ to compute voltage stability margins

1) From the current operating point (base case) with a power transfer of P_0, specify the load and generation increment schedule, and the load composition (such as constant power factors).
2) Use a conventional power flow program with increasing loads until the Newton-Raphson algorithm no longer converges.
3) Starting from the last converged solution in Step 2, apply the AQ-bus power flow method (19)-(28) to continue the power flow solution by increasing the angle separation $(\theta_1 - \theta_N)$ between the AQ bus and the swing bus until the maximum power transfer $P_{0\max}$ is reached. Typically, the bus with the largest load increase will be selected to be the AQ bus. The base-case voltage stability margin is $P_{0m} = P_{0\max} - P_0$.
4) Specify a set of N_c contingencies to be analyzed.
5) For contingency i, repeat Steps 2 and 3 for the post-contingency system to compute the maximum power transfer $P_{i\max}$ and the voltage stability margin $P_{im} = P_{i\max} - P_0$.
6) Repeat Step 5 for all contingencies $i = 1, 2, \ldots, N_c$.
7) The contingency-based voltage stability margin, measured as additional power delivered to the load until the maximum loadability point, is given by

$$P_m = \min_{i=0,\ldots,N_c} \{P_{i\max}\} \tag{29}$$

Note that for any of the contingencies in Step 5, if the AQ-bus algorithm for P_0 fails to converge, that is, P_0 is not a

feasible solution, then the AQ-bus algorithm can be used to reduce P_0 until a converged power flow solution is obtained. The new power flow solution would then be a voltage secure operating condition.

Also note in Steps 3 and 5 of Algorithm 1, all the capability of the conventional power flow can be used. For example, taps can be adjusted to maintain voltages, and generators exceeding their reactive power capability can be changed to PQ buses from PV buses. Both capabilities are important for finding the proper voltage stability limit.[2]

The advantage of using a conventional power flow algorithm in Step 2 of Algorithm 1 is that it will allow a user to select the AQ bus for Step 3. There are several ways to select the AQ bus: (1) use the bus with the largest load increase (as stated in Step 3 of Algorithm 1), (2) use the bus with the largest rate of decrease of the bus voltage magnitude, or (3) use the bus angle with the largest component in the singular vector of the smallest singular value of J from the last converged solution. Frequently all three will yield the same bus.

It is also possible to solve for voltage stability margins without updating J_R (13). This method can be useful when one wants to avoid changing or reprogramming the Jacobian matrix entries, but it has slower convergence. The load increase condition (19), the generator increase condition (20), and the load power factor condition $Q_\ell = P_\ell \tan\phi_\ell$ are now enforced as fixed values after each power flow iteration has converged.

To be more specific, start from the nominal power flow solution with the load on Bus N at P_0. The angular separation of Bus N and the swing bus is increased without changing any injections. The power flow is solved, and the resulting load at Bus N and the generation at the swing bus are computed. This new value P_N is used to compute the load increase on the other load buses (19), to be balanced by the generations according to (20). These new load and generation values are used to solve for another AQ-bus power flow. The process is repeated until the load and generation proportions are within tolerance. This procedure is summarized is the following algorithm.

Algorithm 2: using unmodified J_R to compute voltage stability margins

1) From the current operating point (base case) with a power transfer of P_0, determine the load and generation increment schedule, and the load composition (such as constant power factor).
2) Use a conventional power flow program with increasing loads until the Newton-Raphson algorithm no longer converges.
3) Starting from the last converged solution in Step 2, apply the AQ-bus power flow algorithm (13) by increasing the angle separation between the AQ bus and the swing bus, to obtain a converged value of load at Bus N as P_N.
4) Update the loads and generations at the other buses according to (19) and (20), respectively, and repeat the power flow solution, until (19) and (20) are satisfied.

[2]Chapter 3 of [7] contains a more detailed discussion of voltage stability margin calculation for equipment reaching their reactive power output limits. At the breaking point, the smallest singular value of the conventional Jacobian matrix may not be exactly zero. The AQ-bus method can still be useful if the regular power flow cannot converge at the breaking point.

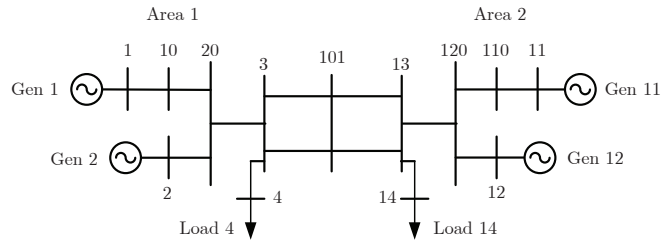

Figure 6. Two-area, four-machine power system

5) Increase the angular separation between Bus N and the swing bus and repeat Steps 3 and 4 until the load power at Bus N reaches the maximum value.
6) Apply Steps 4 to 7 of Algorithm 1 using Steps 2 to 5 of this algorithm to find the contingency-based voltage stability margin.

It is expected that Algorithm 2 would be slower than Algorithm 1. However, in Algorithm 2, minimal additional code for the Jacobian is needed.

IV. Illustrative Examples

In this section the AQ-bus power flow approach is applied to solve for the voltage stability margin of a 2-area, 4-machine system, and a 48-machine system.

A. Two-area system

We first use the Klein-Rogers-Kundur 2-area, 4-machine system [11] shown in Fig. 6 to illustrate the method. In this system, Load 14 will be increased at a constant power factor of 0.9 lagging whereas Load 4 is kept constant at $9.76+j1$ p.u. The load increase is supplied by Generator 1. It is assumed that all the generators have unlimited reactive power supply.

Using Algorithm 1, the conventional power flow solution is shown as the black dashed line of the PV curve in Fig. 7. It fails to converge when the active power of Load 14 is $P_{14} = 19.15$ pu which occurs when the angle separation is $\theta_1 - \theta_{14} = 91.1°$. After this point, the AQ-bus approach is used to continue the power flow solution by further increasing the angle separation between Buses 1 and 14. The solution of the AQ-bus approach is shown as the solid line of the PV curve in Fig. 7. From the PV curve, the critical voltage is 0.8144 p.u. and the maximum active load power is 19.2 p.u., with a power factor of 0.9 lagging.

We also plot the load active power at Bus 14 versus the angle separation $\theta_1 - \theta_{14}$ with the black curves in Fig. 8. Note that at maximum power transfer, $\theta_1 - \theta_{14} = 99.5°$.

1) Singular value analysis: At the maximum loadability point, the largest singular value of J is 423 and the two smallest singular values are 3.59 and 0.02. At the same operating point, the largest and smallest singular values of the $\bar{J}_R$ matrix are 423 and 2.49, respectively. Thus $\bar{J}_R$ does not exhibit any singularity or convergence problems.

At the point where the conventional power flow fails to converge, the smallest singular value of the Jacobian is 0.05 and its singular vector is given in Table II. Note that the element of the singular vector with the largest magnitude corresponds to θ_{14}, the bus angle of the chosen AQ bus.

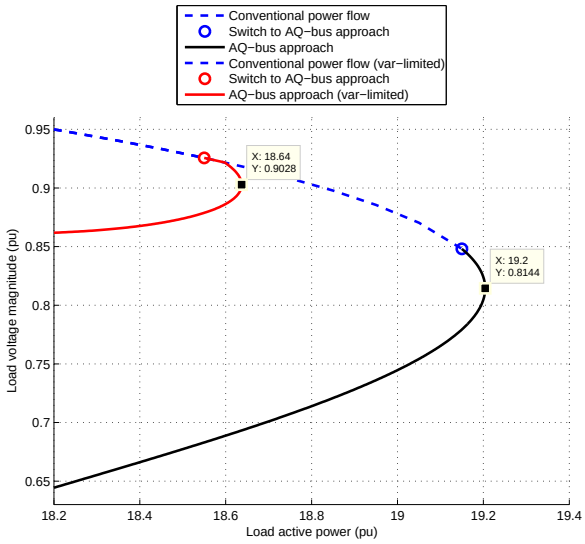

Figure 7. Power-voltage (PV) curves of two-area system, computed using Algorithm 1

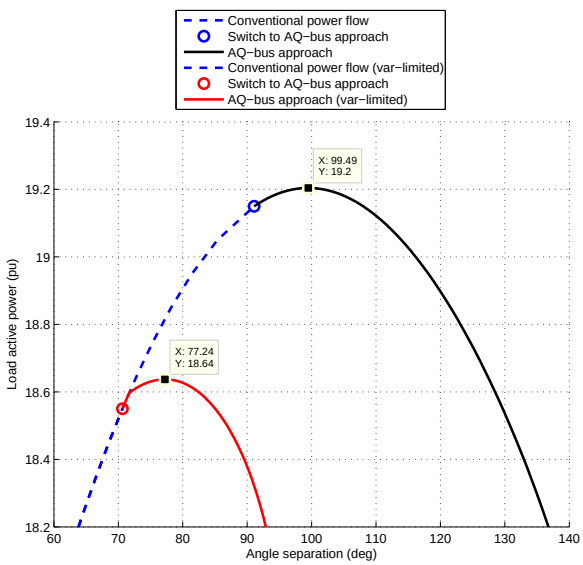

Figure 8. Power-angle ($P\theta$) curves of two-area system, computed using Algorithm 1

2) Including var limits on a generator: Because the AQ-bus power flow incorporates all the functionalities of a conventional power flow, we can readily demonstrate the effect of a var limit on a generator. Suppose we impose a maximum reactive power generation of 3 pu for Generator 2, that is, if the reactive power generation of Generator 2 exceeds 3 pu, it will be changed into a PQ bus with $Q = 3$ pu. The resulting PV and $P\theta$ curves for the same load increase conditions are shown as the red curves in Figs. 7 and 8.

Also of interest is the amount of reactive power provided by the four generators. Fig. 9 shows the reactive power plotted versus $\theta_1 - \theta_{14}$ for the var-limited case. We observe that the var limit on Generator 2 increases the reactive power burden on

Table II
SINGULAR VECTOR CORRESPONDING TO THE SMALLEST SINGULAR VALUE OF THE CONVENTIONAL POWER FLOW JACOBIAN

Singular vector component	Corresponding variable
0.025	θ_2
0.064	θ_3
0.075	θ_4
0.005	θ_{10}
0.329	θ_{11}
0.358	θ_{12}
0.416	θ_{13}
0.450	$\boldsymbol{\theta_{14}}$
0.031	θ_{20}
0.228	θ_{101}
0.332	θ_{110}
0.366	θ_{120}
0.085	V_3
0.086	V_4
0.021	V_{10}
0.117	V_{13}
0.125	V_{14}
0.048	V_{20}
0.172	V_{101}
0.024	V_{110}
0.062	V_{120}

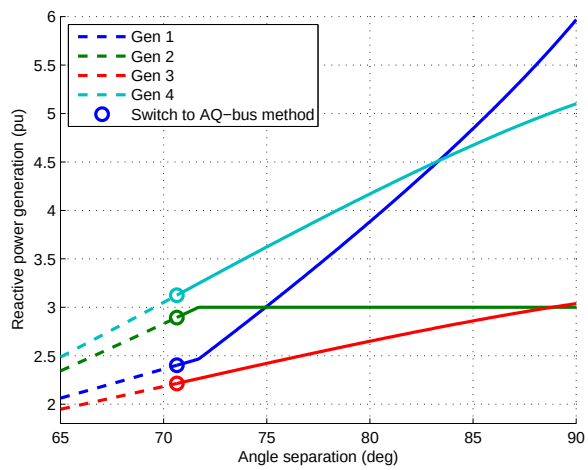

Figure 9. Reactive power output of generators in two-area system with a var limit

Generator 1, and the reactive power losses continue to increase after the point of maximum power transfer point, even though the active power consumed by the load decreases.

3) Solution using Algorithm 2: We applied Algorithm 2 to the two-area system and obtained the same results as with Algorithm 1. Note that with Algorithm 2, J_R is not modified to include the load and generator increase schedules. Thus Algorithm 2 is similar to a dishonest Newton method and needs more iterations than Algorithm 1.

B. NPCC 48-machine system

In this section we extend the AQ-bus power flow to a 48-machine NPCC (Northeast Power Coordinating Council) system [12] using Algorithm 1. A portion of the system map is given in Figure 10. For this system, we increase the loads on

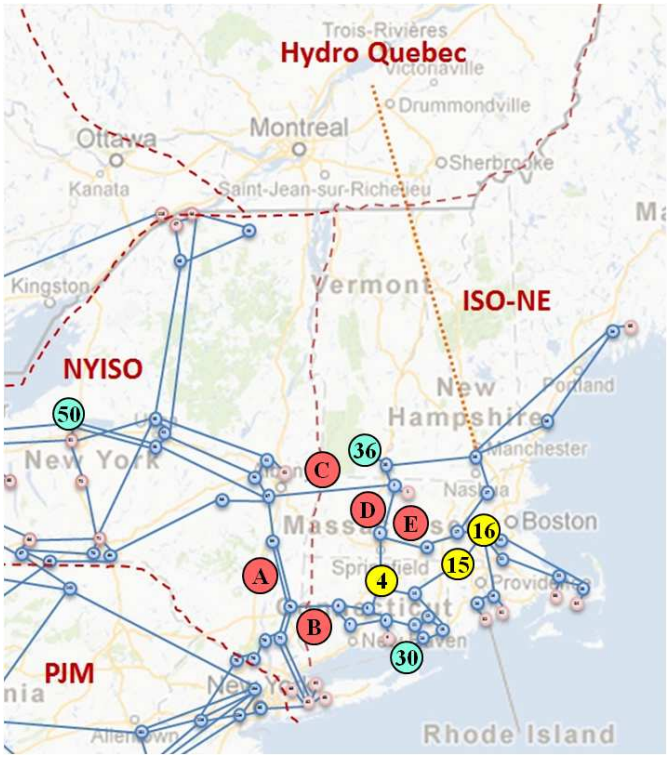

Figure 10. Map of the NPCC 48-machine system

Buses 4, 15, and 16 near Boston, with increased supply coming from the generators on Buses 30 and 36 in New England, and the generator on Bus 50 in New York, as indicated in Fig. 10. We choose Bus 50 as the swing bus and Bus 16 as the AQ bus. Generators on Buses 30 and 36 supply additional power as linear functions of the swing bus power output, as shown in Table III. Similarly, the loads on Buses 4 and 15 are scaled with respect to the AQ bus, as shown in Table IV.[3] The loads at Buses 4, 15, and 16 all have a constant power factor of 0.95 lagging. All the other loads remain constant at their base values, and the active power generation for the other generators also remain constant.

Table III
GENERATOR SCHEDULE FOR 48-MACHINE SYSTEM

Generator Bus #	Bus Type	β_k
50	AV (swing)	-
30	PV	0.10
36	PV	0.80

Table IV
LOAD SCHEDULE FOR 48-MACHINE SYSTEM

Load Bus #	Bus Type	α_ℓ
16	AQ	-
4	PQ	0.50
15	PQ	0.25

We use the AQ-bus method to compute the PV curve for the base case, which is shown in Fig. 11 as the base case. The method readily computes the PV curve to the maximum loadability point and beyond. The algorithm fails to converge when the system voltage is too low, because some load buses can no longer receive enough reactive power.

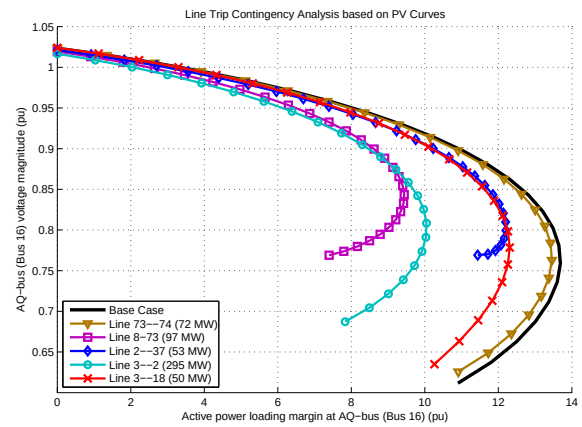

Figure 11. PV-curves for multiple contingencies on the NPCC 48-machine system

To demonstrate the computation of the voltage stability margin for contingency analysis, a set of line outage contingencies (A-E) is selected, as listed in Table V. The location of these lines are labeled in Fig. 10. In Fig. 11, we plot the computed PV curves for the five contingencies against the base case PV curve. Note that each power flow solution is designated with a plot marker in Fig. 11, demonstrating that the AQ-bus method does not require a small step size near the maximum power transfer point. In this example we used a step size of 5° but larger angle steps can be used.

Note that Line 73-74 is in New York. Hence its outage results in a PV curve not much different from the base case PV curve. Lines 3-2 and 3-18 are near the buses with load increases, and thus the PV curves resulting from their outage show less stability margins. Lines 8-73 and 2-37 are interface lines between New York and New England. Their outages have significant impact on the voltage stability margin because part of the load increase in New England is supplied by a New York generator. From Table V, the contingency-based voltage stability margin is 944 MW for the load on Bus 16.

Table V
CONTINGENCY LIST FOR 48-MACHINE SYSTEM

Contingency	Line Outage	Pre-contingency Power Flow	Voltage Stability Margin
A	73–74	72 MW	$1,346$ MW
B	8–73	97 MW	944 MW
C	2–37	53 MW	$1,221$ MW
D	3–2	295 MW	$1,005$ MW
E	3–18	50 MW	$1,231$ MW

V. CONCLUSIONS

In this paper, we have developed a general-purpose power flow method that directly eliminates the matrix singularity issues that arise in PV curve calculations by introducing a new

[3]Any of the buses in the load increase group (Buses 4, 15, and 16) can chosen as the AQ bus for our method to work.

AQ-bus type. The elimination of the singularity using the AQ-bus method was motivated using a classical two-bus system, and a framework was developed to include multiple load buses and multiple generators in the computation of PV curves. We presented two algorithms for practical implementation of the method and demonstrated both algorithms on a small two-area system. Finally, we extended the method to a 48-machine system to show its scalability and applicability to steady-state voltage stability margin calculation and contingency analysis.

This new method provides many advantages in the computation of steady-state voltage stability margins because it does not have numerical issues at the maximum power transfer point. Thus, power system operators can calculate the stability margins using this method far more reliably and quickly than a conventional power flow method.

Acknowledgment

This work was supported in part by the DOE/CERTS award 7040520 and in part by the Engineering Research Center Program of the National Science Foundation and the Department of Energy under NSF Award Number EEC-1041877 and the CURENT Industry Partnership Program. We like to thank DOE project managers Dejan Sobajic, Joe Eto, and Phil Overholt for their support.

References

[1] A. Kurita and T. Sakurai, "The power system failure on July 23, 1987 in Tokyo," in *Proc. of the 27th Conf. on Decision and Control*, 1988.

[2] F. Bourgin, G. Testud, B. Heilbronn, and J. Verseille, "Present Practices and Trends on the French Power System to Prevent Voltage Collapse," *IEEE Transactions on Power Systems*, vol. 8, no. 3, pp. 778–788, 1993.

[3] G. Andersson, P. Donalek, R. Farmer, N. Hatziargyriou, I. Kamwa, P. Kundur, N. Martins, J. Paserba, P. Pourbeik, J. Sanchez-Gasca, R. Schulz, A. Stankovic, C. Taylor, and V. Vittal, "Causes of the 2003 major grid blackouts in North America and Europe, and recommended means to improve system dynamic performance," *IEEE Transactions on Power Apparatus and Systems*, vol. 20, no. 4, pp. 1922–1928, November 2005.

[4] C. Taylor, *Power System Voltage Stability*. New York: McGraw-Hill, 1994.

[5] T. Van Cutsem and C. Vournas, *Voltage Stability of Electric Power Systems*. New York: Springer Science+Business Media, 1998.

[6] K. Iba, H. Suzuki, M. Egawa, and T. Watanabe, "Calculation of critical loading condition with nose curve using homotopy continuation method," *IEEE Transactions on Power Systems*, vol. 6, no. 2, pp. 584–593, 1991.

[7] V. Ajjarapu, *Computational Techniques for Voltage Stability Assessment and Control*. New York: Springer Science+Business Media, 2006.

[8] H.-D. Chiang, A. Flueck, K. Shah, and N. Balu, "CPFLOW: a practical tool for tracing power system steady-state stationary behavior due to load and generation variations," *IEEE Transactions on Power Systems*, vol. 10, no. 2, pp. 623–634, 1995.

[9] Y. Guo, B. Zhang, W. Wu, Q. Guo, and H. Sun, "Solvability and Solutions for Bus-Type Extended Load Flow," *Electrical Power and Energy Systems*, vol. 51, pp. 89–97, 2013.

[10] B. Stott, "Review of load-flow calculation methods," *Proceedings of the IEEE*, vol. 62, no. 7, pp. 916–929, 1974.

[11] M. Klein, G.J. Rogers, and P. Kundur, "A fundamental study of inter-area oscillations in power systems," *IEEE Transactions on Power Systems*, vol. 6, pp. 914–921, Aug. 1991.

[12] J. H. Chow, R. Galarza, P. Accari, and W. Price, "Inertial and slow coherency aggregation algorithms for power system dynamic model reduction," *IEEE Trans. on Power Systems*, vol. 10, no. 2, pp. 680–685, 1995.

Scott G. Ghiocel (S'08) is a postdoctoral research fellow at the Center for Future Energy Systems at Rensselaer Polytechnic Institute. He received his PhD degree in Electrical Engineering from RPI in 2013. His research interests include power system dynamics, voltage stability, and applications of synchronized phasor measurements.

Joe H. Chow (F'92) received his BS degrees in Electrical Engineering and Mathematics from the University of Minnesota, Minneapolis, and MS and PhD degrees, both in Electrical Engineering, from the University of Illinois, Urbana-Champaign. After working in the General Electric power system business in Schenectady, New York, he joined Rensselaer Polytechnic Institute in 1987, and is a professor of Electrical, Computer, and Systems Engineering. His research interests include multivariable control, power system dynamics and control, voltage-source converter-based FACTS controllers, and synchronized phasor data.